



Electrochemical nitrogen atom insertion enabled by a manganese complex†

 Minki Jeon, Pooja Kumari Jat, Juyoung Baek, Geon Kang,  Jaejeong Kim and Isaac Choi *

 Cite this: *Chem. Commun.*, 2026, 62, 7776

 Received 12th January 2026,
Accepted 24th March 2026

DOI: 10.1039/d6cc00221h

rsc.li/chemcomm

Herein, we report a manganaelectrooxidative nitrogen atom insertion, supported by mechanistic studies, exhibiting broad functional group tolerance.

In recent years, skeletal editing has emerged as a groundbreaking platform in molecular engineering,¹ and significant progress has been clearly witnessed.² Indeed, this innovative synthetic toolbox enables chemists to achieve a highly streamlined synthetic process when late-stage reconstruction of molecular frameworks is required.³ Within the realm of skeletal editing, nitrogen insertion has been generally realized by the oxidation-induced C=C bond cleavage. Following key early examples in the 20th century,⁴ recent contributions by Morandi,⁵ Levin,⁶ and Leonori,⁷ among others,⁸ have established the modular assembly of nitrogen-containing heterocycles (Fig. 1A). Transition metal catalysts have also shown promise for nitrogen insertion, though reports on such reactions remain sparse.⁹ However, these reactions typically rely on suprachemometric amounts of terminal oxidants or pre-oxidized precursors under relatively harsh conditions.

Recently, there has been growing interest in electrochemical organic synthesis, which provides chemists with an environmentally benign method for constructing molecules.¹⁰ In this synthetic strategy, an applied electrical potential drives electron flow, specifically enabling oxidation processes at electrode surfaces. Thus, electricity facilitates oxidative chemical transformations through anodic events, thereby avoiding the need for expensive or toxic chemical oxidants. In this context, Cheng,¹¹ Ackermann,¹² and Koh¹³ independently reported nitrogen atom insertion reactions under electrochemical settings (Fig. 1B). Indeed, the strategic selection of readily accessible nitrogen sources, such as ammonia or ammonium carbamate, significantly enhances the efficiency and practicality of the reaction manifold, while the use of external chemical oxidants is rendered unnecessary.

Based on these precedent studies, we envisaged that manganese could be an ideal candidate for a sustainable electrochemical nitrogen insertion reaction with its low toxicity and abundance. Importantly, in recent reports of the Lin group, manganese(II) catalysts play a pivotal role in electrochemical diazidation of C=C bonds.¹⁴ Inspired by these studies, we hypothesized that manganese could serve as an effective platform to control reactivity through ligand modification, thereby enabling nitrogen-atom insertion in place of the well-established diazidation process in the presence of azides under electrochemically oxidative conditions (Fig. 1C).

As a result, we have established a novel electrochemical nitrogen-atom insertion reaction using a manganese complex. Salient features of our strategy include (a) detailed screening of well-defined manganese complexes, (b) preliminary mechanistic investigations to understand the *modus operandi* of present work, and (c) a wide range of functional group tolerance.

We set out to explore optimal reaction conditions for the electrochemical nitrogen insertion into indene **1a** with TMSN₃ as a nitrogen source in the presence of a manganese complex in an undivided cell setup (Scheme 1A and Table S1–S5). Initial experiments (entries 1 and 2) indicated that while diazidation indeed occurred,^{14b} isoquinoline **2a** was afforded as a major product. To enhance operational simplicity, the reaction was conducted under air, which resulted in a slight improvement in the product yield (entry 3). However, under MeCN/AcOH solvent conditions, the cell resistance was measured to be high. Although LiClO₄ was employed as the electrolyte to alleviate this issue, severe passivation of the electrode surface was observed (Table S1). Solvent screening revealed that replacing MeCN with MeOH led to predominant formation of **2a** with low resistance, although diazidation byproduct **3a** and nitrile derivative **4a** slightly increased (entry 4). Interestingly, the addition of molecular sieves and a base improved the yield while suppressing byproducts (entry 5).

Control experiments confirmed the essential role of electro-oxidation process and the need for milder conditions (entries 6–7). These results indirectly suggest that under air atmosphere, molecular oxygen exerts a greater influence on downstream chemical

Department of Chemistry, Chungbuk National University, Chungcheongbuk-do, 28644, Republic of Korea. E-mail: isaac.choi@chungbuk.ac.kr

† Dedicated to Professor Chulbom Lee on the occasion of his 60th birthday.



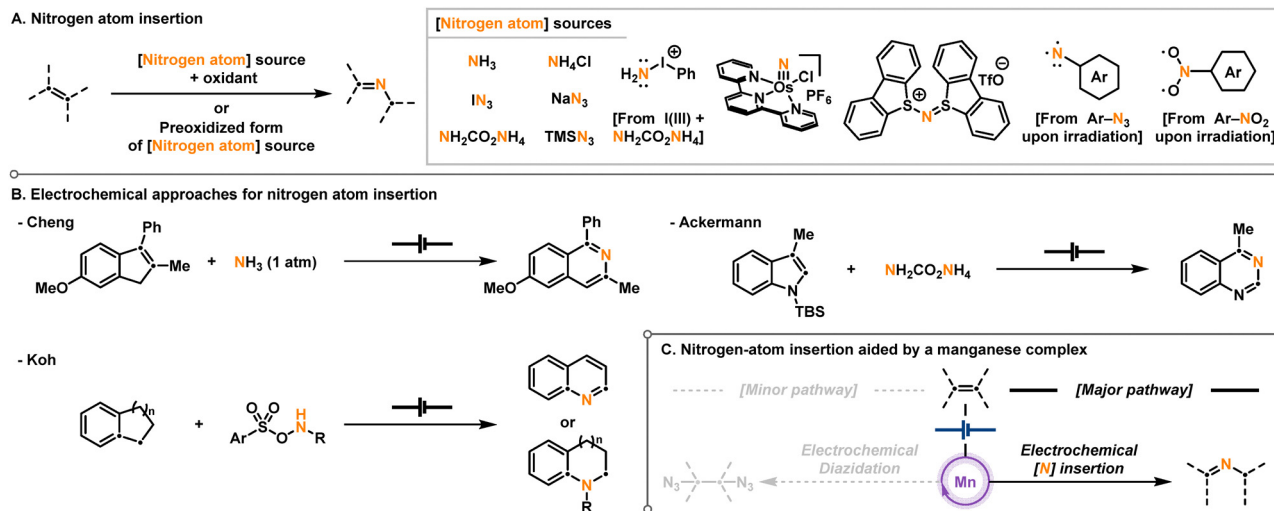


Fig. 1 Background and motivation of the present study. (A) General strategy for nitrogen atom insertion. (B) Recent studies on electrochemical nitrogen atom insertion. (C) Inspiration for the current work.

processes in the reaction manifold rather than serving as a terminal oxidant for Mn(II) species.¹⁵ Finally, a range of manganese complexes ([Mn-1]–[Mn-5]) was evaluated (entry 8, Scheme 1A and Scheme S2), and the bathocuproine ligand exhibited the highest catalytic efficiency, affording **2a** in 70% yield (entry 5, Scheme 1).

Based on the observed reactivity for nitrogen-atom insertion, we sought to elucidate its mechanistic features. To this end, a potentiodynamic electrochemical approach was employed (Scheme 1Bi and Scheme S3–S13). In cyclic voltammetry, the anodic wave of **1a** near 1.0 V shifts to more positive potentials in the presence of manganese with a change in peak shape, indicating that manganese influences the electrochemical oxidation of **1a**. Furthermore, in the potential region above approximately 1.25 V, the anodic current of green trace decreases relative to that observed for **1a** alone, suggesting that manganese species may alter the oxidation pathway of **1a**. Additionally, CV studies with increasing the concentration of TMSN₃ do not lead to a meaningful change in current density (Scheme S14–S17), indicating that direct capture of the electrochemically generated radical cation of **1a** by azide anion is unlikely to be operative. Consistently, no product formation is observed in the absence of [Mn-1] (Scheme 1Bii). Furthermore, when [Mn-6] and [Mn-7] were subjected to the electrochemical reaction conditions (Scheme 1Bii), product formation was observed, albeit with slightly reduced efficiency. Additionally, CV studies of the [Mn-6] clearly demonstrate that the *in situ* generated Mn(II)–N₃ species is involved in the catalytic system under the electrooxidative conditions (Scheme S18).

To gain more detailed insight, the reaction with **1b** was profiled under a series of applied cell voltages ranging from 1.0 to 2.0 V (Scheme 1Ci). The initial rate shows a linear dependence on the applied potential, implying that catalytic turnover is sensitive to the electrochemical driving force. Also, extrapolation of the rate-potential relationship toward lower potentials suggests productive electrocatalysis ceases at approximately 0.7 V. Consistent with this analysis, constant-potential electrolysis (CPE) at 0.6 V produced no detectable product while the starting material was also fully consumed, likely due to unproductive direct oxidation (Scheme 1Cii).

In contrast, electrolysis at 1.0 V afforded the desired products. These results are consistent with CV studies shown in Scheme 1Bi (green trace), in which onset potential of the reaction mixture is observed at approximately 0.67 V, highlighting the crucial role of manganese catalyst in enabling the electrochemical nitrogen atom insertion.

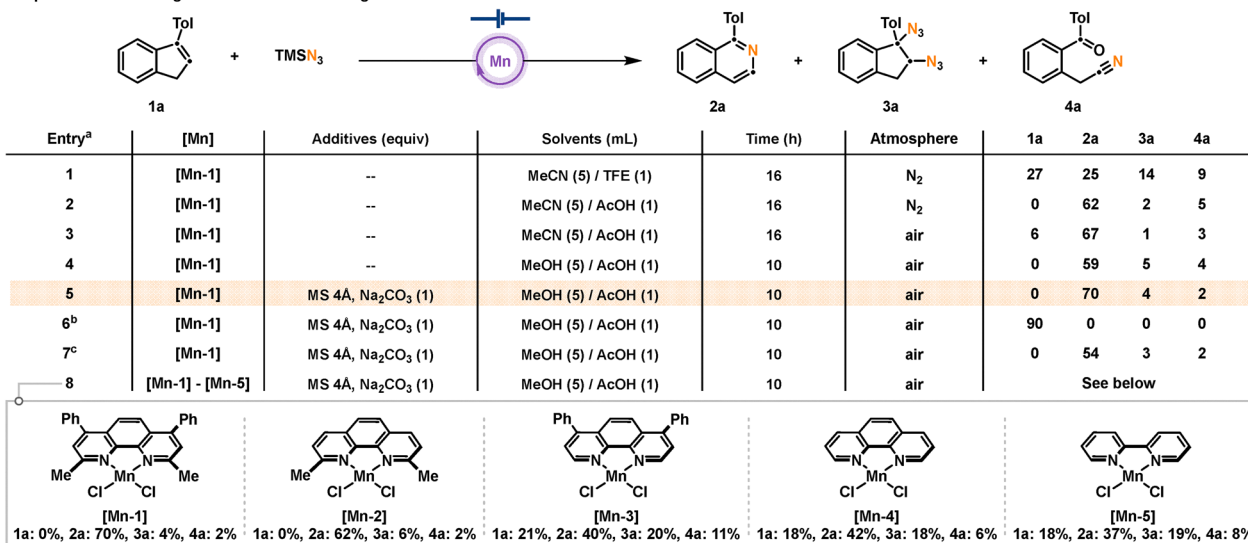
With a mechanistic understanding in hand, the scope of the manganese-catalyzed electrochemical nitrogen-atom insertion was explored (Scheme 2A). A series of differently substituted 1-arylisquinolines **2** was afforded, revealing that not only electron-withdrawing substituents but also electron donating groups were fully tolerated under the optimized conditions. Importantly, in the case of a substrate bearing a styrene moiety, a desired product **2j** was solely formed. The C3-substituents on indene is not required (**2l–2m**), and the method was also successfully applied to the synthesis of pyridines (**2n–2p**). Furthermore, the developed protocol could be extended to the synthesis of a pharmaceutical compound, Perampanel (**2q**), and a derivative of a natural product, Pterostilbene (**2r**). Interestingly, a reaction with a radical probe **1s** resulted in the formation of nitrogen-inserted product **2s**, while a ring opened product was not detected (Scheme 2B).^{15,16}

On the basis of our mechanistic insights, a plausible pathway for manganese-catalyzed electrochemical nitrogen atom insertion is proposed (Scheme 2C). Initially, the *in situ* generated Mn(II)–N₃ complex undergoes anodic oxidation, thereby affording an azide radical. The resulting azide radical reacts with substrate **1a** to generate intermediate **A**, which subsequently undergoes annulation to form the aziridine radical intermediate **B**.^{9c} This species then undergoes intramolecular rearrangement followed by oxidative aromatization to furnish the final product **2a**.

In conclusion, we have established a manganese-catalyzed electrocatalytic strategy for nitrogen incorporation into unsaturated frameworks that proceeds under mild conditions without the use of external oxidants. Mechanistic experiments indicate the participation of manganese–azide intermediates which is competent to generate azide radical. The reaction displays broad substrate compatibility and accommodates diverse functional groups, thereby offering a



A. Optimization for manganese electrooxidative nitrogen atom insertion

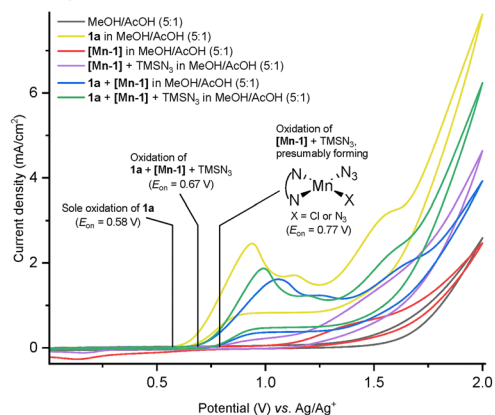


^a Reaction conditions: **1a** (0.2 mmol), TMSN₃ (0.2 mmol), 30 °C, anode: GF, cathode: Pt, $U_{cell} = 1.0$ V. Yields were determined by ¹H NMR with mesitylene as internal standard.

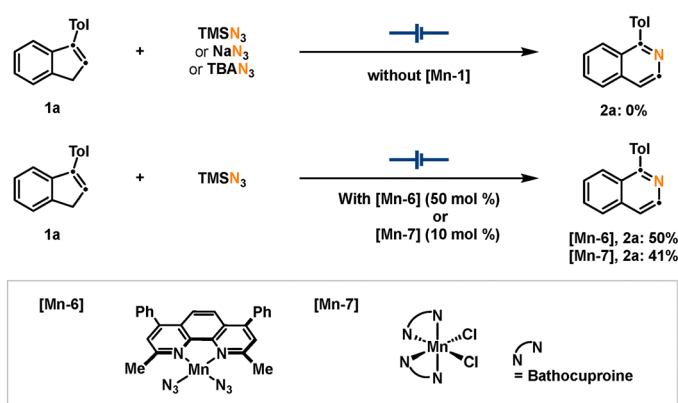
^b No potential. ^c 60 °C. (TFE = 2,2,2-Trifluoroethanol; MS = Molecular sieve; air = No N₂ purging; reaction conducted in a closed flask.)

B. Cyclic voltammetric study^a and preliminary mechanistic investigations

i. CV analysis



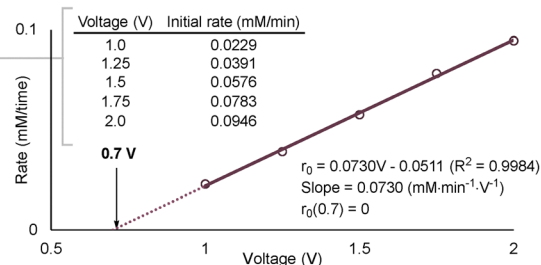
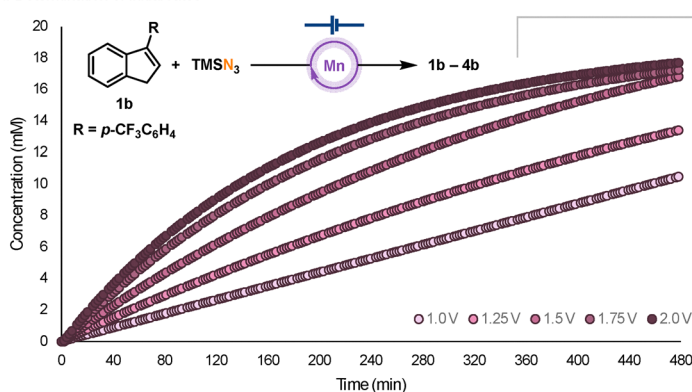
ii. Control experiments



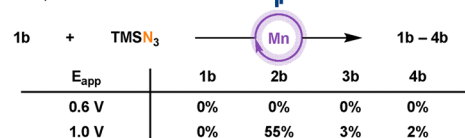
^a Working electrode = GC disk (3 mm); Counter electrode = coiled Pt wire; Reference electrode = 0.01 M Ag/Ag⁺ (4 mm; Ag wire in 0.01 M AgNO₃ / 0.1 M TBAPF₆ in MeCN); Solution = 0.1 M TBAPF₆; Mn complex = 1 mM in 0.1 M TBAPF₆; analyte = 4 mM in 0.1 M TBAPF₆; Scan rate = 100 mV/s.

C. Potential-dependence analysis and constant potential electrolysis experiments

i. Determination of initial rates

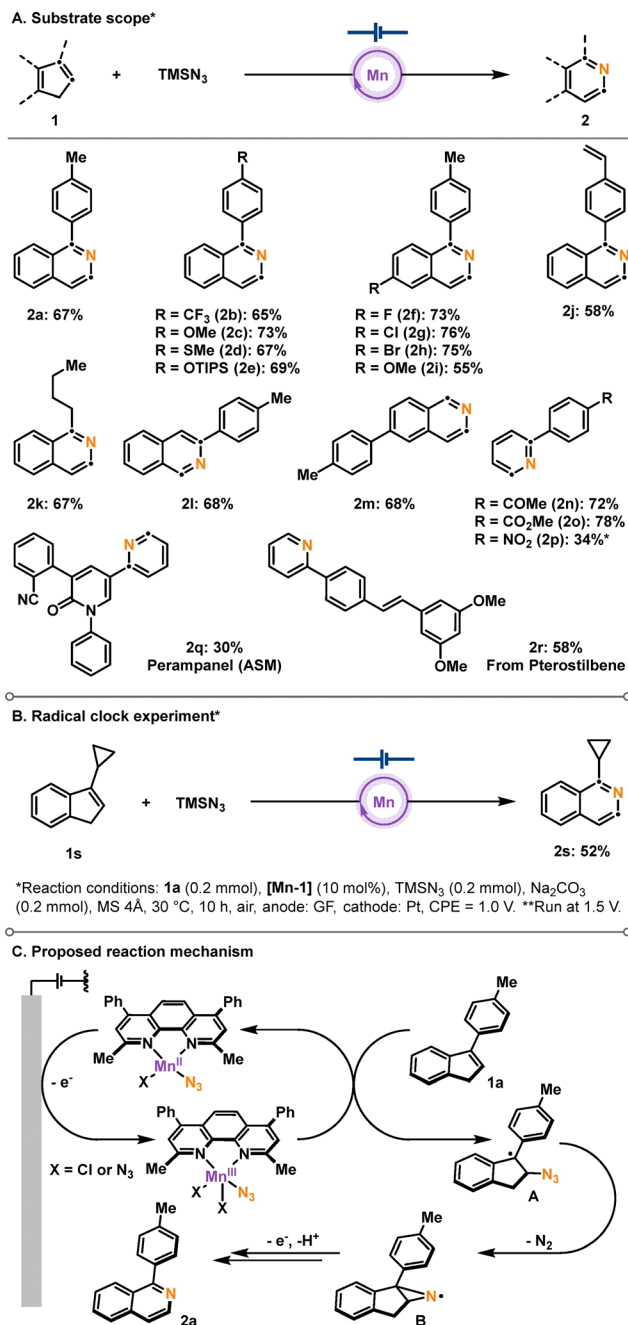


ii. CPE experiments



Scheme 1 Optimization and mechanistic studies. (A) Selective transformation enabling nitrogen atom insertion. (B) Potentiodynamic and complementary experimental analyses. (C) Preliminary kinetic studies.





Scheme 2 Substrate scope and radical clock experiment. (A) Versatility in manganese-catalyzed electrochemical nitrogen atom insertion. (B) Radical pathway determination. (C) Proposed reaction mechanism.

practical and environmentally benign approach for constructing nitrogen-containing molecular architectures.

MJ: investigation, formal analysis, data curation, visualization, writing – original draft; PKJ: investigation; JB: investigation; GK: investigation; JK: investigation; IC: conceptualization, supervision, project administration, funding acquisition, writing – review & editing.

I. C. and the Choi group thank MSIT, MOE, NRF, and CBNU. This work was supported by the National Research Foundation of Korea (NRF) grant, funded by the Korea government (MSIT)

(No. RS-2023-00210101) and the Global Learning & Academic Research Institution for Master's-PhD Students, and Postdocs (G-LAMP) Program of the NRF grant funded by the Ministry of Education (No. RS-2024-00445180). This work was supported by a funding for the academic research program of Chungbuk National University in 2025.

Conflicts of interest

There are no conflicts to declare.

Data availability

The data supporting this article have been included as part of the supplementary information (SI). Supplementary information includes experimental procedures, details of kinetic studies, and analytical data. See DOI: <https://doi.org/10.1039/d6cc00221h>.

References

- (a) M. D. Levin, *Synlett*, 2024, 35, 1471–1474; (b) J. Jurczyk, J. Woo, S. F. Kim, B. D. Dherange, R. Sarpong and M. D. Levin, *Nat. Synth.*, 2022, 1, 352–364; (c) B. Iddon, O. Meth-Cohn, E. F. V. Scriven, H. Suschitzky and P. T. Gallagher, *Angew. Chem., Int. Ed. Engl.*, 1979, 18, 900–917.
- (a) F.-P. Wu, C. C. Chintawar, R. Lalisce, P. Mukherjee, S. Dutta, J. Tyler, C. G. Daniliuc, O. Gutierrez and F. Glorius, *Nat. Catal.*, 2024, 7, 242–251; (b) J. Masson-Makdissi, R. F. Lalisce, M. Yuan, B. D. Dherange, O. Gutierrez and M. D. Levin, *J. Am. Chem. Soc.*, 2024, 146, 17719–17727; (c) S. F. Kim, H. Schwarz, J. Jurczyk, B. R. Nebgen, H. Hendricks, H. Park, A. Radosevich, M. W. Zuerch, K. Harper, M. C. Lux, C. S. Yeung and R. Sarpong, *J. Am. Chem. Soc.*, 2024, 146, 5580–5596; (d) G. L. Bartholomew, S. L. Kraus, L. J. Karas, F. Carpaneto, R. Bennett, M. S. Sigman, C. S. Yeung and R. Sarpong, *J. Am. Chem. Soc.*, 2024, 146, 2950–2958; (e) B. A. Wright, A. Matviitsuk, M. J. Black, P. Garcia-Reynaga, L. E. Hanna, A. T. Herrmann, M. K. Ameriks, R. Sarpong and T. P. Lebold, *J. Am. Chem. Soc.*, 2023, 145, 10960–10966; (f) J. Woo, C. Stein, A. H. Christian and M. D. Levin, *Nature*, 2023, 623, 77–82; (g) B. D. Dherange, M. Yuan, C. B. Kelly, C. A. Reiher, C. Grosanu, K. J. Berger, O. Gutierrez and M. D. Levin, *J. Am. Chem. Soc.*, 2023, 145, 17–24; (h) J. Woo, A. H. Christian, S. A. Burgess, Y. Jiang, U. F. Mansoor and M. D. Levin, *Science*, 2022, 376, 527–532; (i) E. E. Hyland, P. Q. Kelly, A. M. McKillop, B. D. Dherange and M. D. Levin, *J. Am. Chem. Soc.*, 2022, 144, 19258–19264; (j) G. L. Bartholomew, F. Carpaneto and R. Sarpong, *J. Am. Chem. Soc.*, 2022, 144, 22309–22315; (k) S. H. Kennedy, B. D. Dherange, K. J. Berger and M. D. Levin, *Nature*, 2021, 593, 223–227; (l) J. Jurczyk, M. C. Lux, D. Adressa, S. F. Kim, Y.-H. Lam, C. S. Yeung and R. Sarpong, *Science*, 2021, 373, 1004–1012; (m) B. D. Dherange, P. Q. Kelly, J. P. Liles, M. S. Sigman and M. D. Levin, *J. Am. Chem. Soc.*, 2021, 143, 11337–11344; (n) K. J. Berger, J. L. Driscoll, M. Yuan, B. D. Dherange, O. Gutierrez and M. D. Levin, *J. Am. Chem. Soc.*, 2021, 143, 17366–17373.
- (a) S. Wiesler, G. Sennari, M. V. Popescu, K. E. Gardner, K. Aida, R. S. Paton and R. Sarpong, *Nat. Commun.*, 2024, 15, 4125; (b) S. Holovach, K. P. Melnykov, I. Poroshyn, R. T. Iminov, D. Dudenko, I. Kondratov, M. Levin and O. O. Grygorenko, *Chem. – Eur. J.*, 2023, 29, e202203470; (c) T. Hosoya, T. Hiramatsu, T. Ikemoto, M. Nakanishi, H. Aoyama, A. Hosoya, T. Iwata, K. Maruyama, M. Endo and M. Suzuki, *Org. Biomol. Chem.*, 2004, 2, 637–641.
- (a) A. Albini, G. Bettinetti and G. Minoli, *J. Am. Chem. Soc.*, 1997, 119, 7308–7315; (b) K. Narasimhan and P. R. Kumar, *Heterocycles*, 1984, 22, 1369–1375; (c) D. S. Dime and S. McLean, *J. Org. Chem.*, 1981, 46, 4999–5000; (d) R. B. Miller and J. M. Frincke, *J. Org. Chem.*, 1980, 45, 5312–5315; (e) M. Ikeda, F. Tabusa, Y. Nishimura, S. Kwon and Y. Tamura, *Tetrahedron Lett.*, 1976, 17, 2347–2350; (f) M. I. Fremery and E. K. Fields, *J. Org. Chem.*, 1964, 29, 2240–2243.



- 5 (a) A.-S. K. Paschke, E. J. Meeus, M. A. Masota, F. Hoffmann, N. M. Grob and B. Morandi, *J. Am. Chem. Soc.*, 2026, **148**, 55–60; (b) J. C. Reisenbauer, A.-S. K. Paschke, J. Krizic, B. B. Botlik, P. Finkelstein and B. Morandi, *Org. Lett.*, 2023, **25**, 8419–8423; (c) P. Finkelstein, J. C. Reisenbauer, B. B. Botlik, O. Green, A. Florin and B. Morandi, *Chem. Sci.*, 2023, **14**, 2954–2959; (d) J. C. Reisenbauer, O. Green, A. Franchino, P. Finkelstein and B. Morandi, *Science*, 2022, **377**, 1104–1109.
- 6 (a) T. J. Pearson, R. Shimazumi, J. L. Driscoll, B. D. Dherange, D.-I. Park and M. D. Levin, *Science*, 2023, **381**, 1474–1479; (b) P. Q. Kelly, A. S. Filatov and M. D. Levin, *Angew. Chem., Int. Ed.*, 2022, **61**, e202213041.
- 7 (a) R. Mykura, R. Sánchez-Bento, E. Matador, V. K. Duong, A. Varela, L. Angelini, R. J. Carbajo, J. Llaveria, A. Ruffoni and D. Leonori, *Nat. Chem.*, 2024, **16**, 771–779; (b) R. Sánchez-Bento, B. Roure, J. Llaveria, A. Ruffoni and D. Leonori, *Chemistry*, 2023, **9**, 3685–3695; (c) E. Matador, M. J. Tilby, I. Saridakis, M. Pedrón, D. Tomczak, J. Llaveria, I. Atodiresei, P. Merino, A. Ruffoni and D. Leonori, *J. Am. Chem. Soc.*, 2023, **145**, 27810–27820; (d) A. Ruffoni, C. Hampton, M. Simonetti and D. Leonori, *Nature*, 2022, **610**, 81–86.
- 8 (a) X.-X. Zhang, S.-T. Xu, X.-T. Li, T.-T. Song, D.-W. Ji and Q.-A. Chen, *J. Am. Chem. Soc.*, 2025, **147**, 11533–11542; (b) E. Z. Schroeder, C. Lin, Y. Hu, Z.-Y. Dai, A. F. Griffin, T. S. Hotvedt, I. A. Guzei and J. M. Schomaker, *J. Am. Chem. Soc.*, 2024, **146**, 22085–22092; (c) A. Lin, A. Ghosh, S. Yellen, Z. T. Ball and L. Kürti, *J. Am. Chem. Soc.*, 2024, **146**, 21129–21136; (d) C. Amber, L. T. Göttemann, R. T. Steele, T. M. Petitjean and R. Sarpong, *J. Org. Chem.*, 2024, **89**, 17655–17663; (e) G. Li, M. N. Lavagnino, S. Z. Ali, S. Hu and A. T. Radosevich, *J. Am. Chem. Soc.*, 2023, **145**, 41–46; (f) S. C. Patel and N. Z. Burns, *J. Am. Chem. Soc.*, 2022, **144**, 17797–17802; (g) F. R. Bou-Hamdan, F. Lévesque, A. G. O'Brien and P. H. Seeberger, *Beilstein J. Org. Chem.*, 2011, **7**, 1124–1129.
- 9 (a) Z. Wang, H. Xu, X. Han, S. Fan and J. Zhu, *Org. Lett.*, 2024, **26**, 8559–8564; (b) T. Heilmann, J. M. Lopez-Soria, J. Ulbrich, J. Kircher, Z. Li, B. Worbs, C. Golz, R. A. Mata and M. Alcarazo, *Angew. Chem., Int. Ed.*, 2024, **63**, e202403826; (c) J. Wang, H. Lu, Y. He, C. Jing and H. Wei, *J. Am. Chem. Soc.*, 2022, **144**, 22433–22439; (d) M.-M. Xu, W.-B. Cao, X.-P. Xu and S.-J. Ji, *Chem. Commun.*, 2018, **54**, 12602–12605.
- 10 (a) N. E. S. Tay, D. Lehnher and T. Rovis, *Chem. Rev.*, 2022, **122**, 2487–2649; (b) K.-J. Jiao, Z.-H. Wang, C. Ma, H.-L. Liu, B. Cheng and T.-S. Mei, *Chem Catal.*, 2022, **2**, 3019–3047; (c) H. Huang, K. A. Steiniger and T. H. Lambert, *J. Am. Chem. Soc.*, 2022, **144**, 12567–12583; (d) L. F. T. Novaes, J. Liu, Y. Shen, L. Lu, J. M. Meinhardt and S. Lin, *Chem. Soc. Rev.*, 2021, **50**, 7941–8002; (e) K. Yamamoto, M. Kuriyama and O. Onomura, *Acc. Chem. Res.*, 2020, **53**, 105–120; (f) C. Schotten, T. P. Nicholls, R. A. Bourne, N. Kapur, B. N. Nguyen and C. E. Willans, *Green Chem.*, 2020, **22**, 3358–3375; (g) C. Kingston, M. D. Palkowitz, Y. Takahira, J. C. Vantourout, B. K. Peters, Y. Kawamata and P. S. Baran, *Acc. Chem. Res.*, 2020, **53**, 72–83; (h) J. E. Kim, S. Choi, M. Balamurugan, J. H. Jang and K. T. Nam, *Trends Chem.*, 2020, **2**, 1004–1019; (i) Q. Jing and K. D. Moeller, *Acc. Chem. Res.*, 2020, **53**, 135–143; (j) G. Hilt, *ChemElectroChem*, 2020, **7**, 395–405; (k) T. Fuchigami and S. Inagi, *Acc. Chem. Res.*, 2020, **53**, 322–334; (l) M. Yan, Y. Kawamata and P. S. Baran, *Angew. Chem., Int. Ed.*, 2018, **57**, 4149–4155; (m) N. Sauermann, T. H. Meyer, Y. Qiu and L. Ackermann, *ACS Catal.*, 2018, **8**, 7086–7103; (n) J.-i. Yoshida, K. Kataoka, R. Horcajada and A. Nagaki, *Chem. Rev.*, 2008, **108**, 2265–2299.
- 11 S. Liu and X. Cheng, *Nat. Commun.*, 2022, **13**, 425.
- 12 B. S. Zhang, S. L. Homolle, T. Bauch, J. C. A. Oliveira, S. Warratz, B. Yuan, X. Y. Gou and L. Ackermann, *Angew. Chem., Int. Ed.*, 2024, **63**, e202407384.
- 13 G.-Q. Sun, X. Wang, R. Hu, W. Rao, Y. Zhao and M. J. Koh, *Nat. Synth.*, 2026, **5**, 466–475.
- 14 (a) L. F. T. Novaes, Y. Wang, J. Liu, X. Riart-Ferrer, W.-C. Cindy Lee, N. Fu, J. S. K. Ho, X. P. Zhang and S. Lin, *ACS Catal.*, 2022, **12**, 14106–14112; (b) N. Fu, G. S. Sauer, A. Saha, A. Loo and S. Lin, *Science*, 2017, **357**, 575–579.
- 15 X. Sun, X. Li, S. Song, Y. Zhu, Y.-F. Liang and N. Jiao, *J. Am. Chem. Soc.*, 2015, **137**, 6059–6066.
- 16 W. Yang, Y. Lan, Y. Bai, Z. Zhao, Y. Song, R. Chang, X. Shang, S. Li, S. Jia, S. Liu, S.-J. Li and L. Niu, *Chemistry*, 2025, **12**, 102702.

